Article

A Suite of H NMR Spin Relaxation Experiments for the Measurement of RNA Dynamics

Pramodh Vallurupalli, and Lewis E. Kay

J. Am. Chem. Soc., **2005**, 127 (18), 6893-6901• DOI: 10.1021/ja0427799 • Publication Date (Web): 19 April 2005

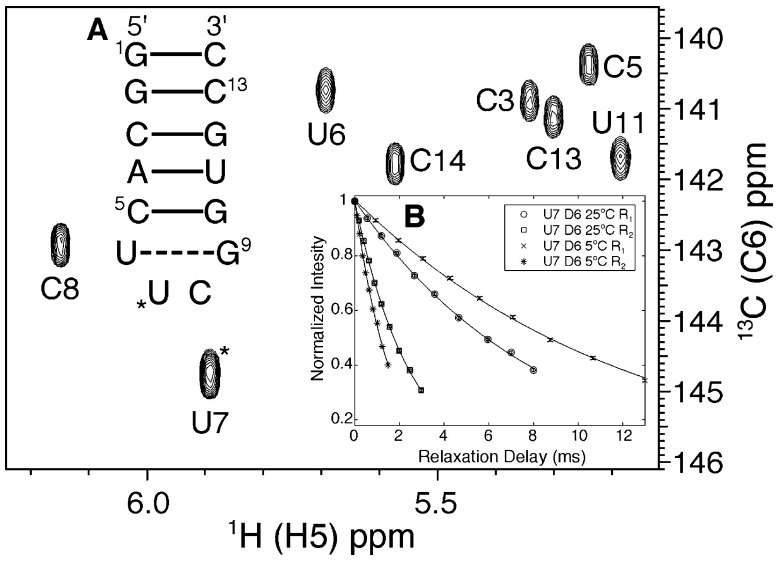

More About This Article

Additional resources and features associated with this article are available within the HTML version:

- Supporting Information
- Links to the 2 articles that cite this article, as of the time of this article download
- Access to high resolution figures
- Links to articles and content related to this article
- Copyright permission to reproduce figures and/or text from this article

View the Full Text HTML

J|A|C|S
ARTICLES
Published on Web 04/19/2005

A Suite of ^{2}H NMR Spin Relaxation Experiments for the Measurement of RNA Dynamics

Pramodh Vallurupalli and Lewis E. Kay*

Contribution from the Protein Engineering Network Centers of Excellence and the Departments of Medical Genetics, Biochemistry and Chemistry, The University of Toronto, Toronto, Ontario, Canada, M5S 1A8

Received November 30, 2004; E-mail: kay@pound.med.utoronto.ca

Abstract: A suite of ^{2}H-based spin relaxation NMR experiments is presented for the measurement of molecular dynamics in a site-specific manner in uniformly ^{13}C, randomly fractionally deuterated (~50%) RNA molecules. The experiments quantify ^{2}H R_1 and R_2 relaxation rates that can subsequently be analyzed to obtain information about dynamics on a pico- to nanosecond time scale. Sensitivity permitting, the consistency of the data can be evaluated by measuring all five rates that are accessible for a spin 1 particle and establishing that the rates obey relations that are predicted from theory. The utility of the methodology is demonstrated with studies of the dynamics of a 14-mer RNA containing the UUCG tetraloop at temperatures of 25 and 5 °C. The high quality of the data, even at 5 °C, suggests that the experiments will be of use for the study of RNA molecules that are as large as 30 nucleotides.

Introduction

Dynamics play a key role in the function of many RNA molecules. For example, the hammerhead and lead dependent ribozymes must undergo conformational changes for function in which a highly populated inactive ground state exchanges with a low populated, active excited state.[1−3] Structures of the ribosome at different stages along the reaction coordinate have established in spectacular fashion that it is a dynamic molecular machine, with significant changes in RNA structure accompanying ligand binding.[4,5] Changes in the structures of RNAs upon binding protein have also been characterized. Binding of U1A to its cognate mRNA leads to a substantial reorganization of the RNA, regulating polyadenylation of the message.[6] Large conformational changes in a three-helix junction region in 16S rRNA accompany binding of the S15 ribosomal protein.[6] It is clear that the dynamics of RNA molecules affect both the specificity and affinity of binding and that site-specific dynamics information is an important complement to static structural data. Unfortunately, to date there has been little methodology development to facilitate such studies.

NMR spectroscopy is an extremely powerful probe of molecular dynamics spanning a wide range of time scales extending over many orders of magnitude.[7] Over the past two decades, methods have been developed to study local dynamics in protein molecules in a site-specific manner, providing insights into molecular recognition, protein thermodynamics, and protein folding.[8] Often studies involve measurement of the relaxation properties of backbone amide ^{15}N spins, exploiting the high resolution of the amide region of ^{15}N−^{1}H correlation maps and the fact that the interactions that contribute to the relaxation of the amide nitrogen are well understood. More recently, backbone ^{13}C spin relaxation experiments have emerged as a powerful complement to the nitrogen studies.[9]

Studies of nucleic acids using ^{15}N or ^{13}C spin relaxation have also been reported, but these applications are much more limited than the corresponding studies involving proteins. In the case of RNA/DNA, ^{15}N studies are generally limited to imino groups,[10] so that the base dynamics of adenine and cytosine (bases that lack N−H moieties) cannot be addressed. Moreover, imino protons exchange rapidly with solvent so that experiments must be performed at low temperatures, and even in this case only those that are stably hydrogen-bonded give rise to observable signals. Finally, an accurate quantification of relaxation rates is predicated on knowledge of the magnitudes (and orientations) of the interactions that contribute to relaxation in the first place; knowledge of the appropriate chemical shift anisotropies (CSAs) for imino nitrogens are semiquantitative at best.[10] An alternative strategy involves measuring ^{13}C spin relaxation properties of methine groups in nucleic acids that

(1) Blount, K. F.; Uhlenbeck, O. C. *Biochem. Soc. Trans.* **2002**, *30*, 1119−1122.
(2) Hoogstraten, C. G.; Legault, P.; Pardi, A. *J. Mol. Biol.* **1998**, *284*, 337−350.
(3) Wedekind, J. E.; McKay, D. B. *Nat. Struct. Biol.* **1999**, *6*, 261−268.
(4) Ogle, J. M.; Carter, A. P.; Ramakrishnan, V. *Trends Biochem. Sci* **2003**, *28*, 259−266.
(5) Green, R.; Noller, H. F. *Annu. Rev. Biochem.* **1997**, *66*, 679−716.
(6) Williamson, J. R. *Nat. Struct. Biol.* **2000**, *7*, 834−837.
(7) Palmer, A. G.; Williams, J.; McDermott, A. *J. Phys. Chem.* **1996**, *100*, 13293−13310.
(8) Stone, M. J. *Acc. Chem. Res.* **2001**, *34*, 379−388.
(9) Wang, T.; Cai, S.; Zuiderweg, E. R. *J. Am. Chem. Soc.* **2003**, *125*, 8639−8643.
(10) Akke, M.; Fiala, R.; Jiang, F.; Patel, D.; Palmer, A. G., III. *RNA* **1997**, *3*, 702−709.

are at natural abundance,[11] fractionally[12] or uniformly ^{13}C labeled.[13] Applications to base carbons are complicated, however, by the requirement for accurate CSA values.

Here we use an alternative strategy that builds upon our previous work in proteins exploiting the deuteron as a spin-spy probe of molecular dynamics.[14,15] Interpretation of the dynamics data is considerably simplified by the fact that the relaxation of the deuteron is exclusively due to the quadrupolar-electric field gradient interaction; analysis of the resultant relaxation data is, therefore, somewhat more straightforward than for data from either ^{15}N or ^{13}C studies. Moreover, unlike for ^{13}C and ^{15}N relaxation, chemical exchange has a negligible effect on ^{2}H transverse relaxation rates because of their large magnitude and the small chemical shift dispersion of ^{2}H spins. This is particularly of relevance in applications involving RNA/DNA since the smaller number of measurements that probe dynamics relative to proteins, coupled with uncertainties in CSA values, often makes it difficult to identify nuclei that are subject to chemical exchange in the first place.

A suite of relaxation experiments is presented for the measurement of ^{2}H R_1,R_2 relaxation rates at the 1′,2′,4′,5′,5″ sugar and 5,6 base (U,C) positions in uniformly ^{15}N, ^{13}C, ∼50% ^{2}H labeled RNA. Many of the experiments involve HCCD "out-and-back" magnetization transfers that are necessary in cases where ^{2}H spin relaxation at methine positions is to be probed; as such the pulse schemes are distinct from experiments that measure ^{2}H relaxation properties of deuterolabeled methyl groups in proteins. The utility of the methodology is illustrated on a small 14-nucleotide stem loop containing the UUCG tetraloop[16] with relaxation data recorded at both 25 and 5 °C and the rates subsequently interpreted using the Lipari−Szabo model free formalism.[17] The applicability of these experiments to larger systems is discussed.

Materials and Methods

Sample Preparation. ^{15}N,^{13}C ∼50% ^{2}H labeled NTPs were isolated from *Methylophilus methylotrophus* grown in 55% $^{2}H_2O$ with ^{13}C methanol and ^{15}N ammonium sulfate as the carbon and nitrogen sources.[18] The RNA sample was transcribed using these NTPs and T7 RNA polymerase from a partially double-stranded DNA template in which the last two nucleotides contained a C2′ methoxy modification[19] and purified by standard techniques.[20] The NMR sample was approximately 2.7 mM in concentration, 20 mM potassium phosphate, and 0.4 mM EDTA, pH 6.4, 100% $^{2}H_2O$.

NMR Spectroscopy and Data Analysis. All the deuterium relaxation experiments on the RNA sample were performed on a 600 MHz Varian Inova spectrometer equipped with a cryogenic probehead. Values of R_1 and R_2 were obtained at 25 and 5 °C with typical acquisition times ranging between 10 and 30 h for each R_1,R_2 data set (see Supporting Information for details). Data processing and analysis were performed with NMRpipe software.[21] Extracted intensities of peak heights were fit to a single exponential of the form $I = I_o \exp(-RT)$, where I is the measured intensity, T is the delay time (see Figure 1), and R is the relaxation rate. Errors in peak intensities were estimated on the basis of repeat measurements (two data sets repeated out of ∼10−12 obtained for each relaxation rate) and subsequently propagated to errors in rates using a Monte Carlo analysis.[22] In cases where calculated errors in rates were less than 2%, an error of 2% was assigned.

Experimental NMR Pulse Sequence Details. Figure 1 illustrates the pulse schemes that have been derived for the measurement of ^{2}H R_1 and R_2 relaxation rates at 1′,2′,4′,5′,5″ sugar and 5,6 base (U,C) positions in uniformly ^{15}N,^{13}C ∼50% ^{2}H labeled RNA. ^{15}N labeling is not a prerequisite for these experiments. Narrow (wide) rectangular pulses correspond to 90° (180°) flip angles. Band selective pulses are denoted by shapes. R_1 and R_2 values are measured by inserting sequences F or G into the boxes denoted by "R_1 or R_2" in parts A−E. The ^{1}H and ^{15}N carriers are placed at 4.7 and 150 ppm, respectively; all ^{1}H, ^{15}N, and ^{13}C pulses indicated by filled rectangles are applied with the highest available power (^{1}H, ^{13}C, and ^{2}H decoupling use 5.8 kHz, 2.2 kHz, and 700 Hz fields, respectively). ^{2}H pulses (90°) are of duration 140 μs. All pulse widths for shaped pulses, pwSH, should be scaled according to pwSH*600/X, where X is the field strength in MHz. Phases, φ_s, of selective pulses are adjusted carefully (and *independently*) to optimize sensitivity. Figure 1A shows the scheme for measurement of relaxation of D5 and D6. The ^{13}C transmitter is at 120 ppm. Pulses indicated by "AR" are applied with the RE-BURP[23] shape (on resonance, 480 μs; care must be taken to ensure that these pulse do not excite base C4 carbons). C4 band selective decoupling (centered at 168.5 ppm, bandwidth of 7 ppm) uses WURST-2 shaped pulses[24] of duration 3 ms. The decoupling scheme was generated with the Varian Pbox tool. The delays used are: $\tau_a = \tau_b = 1.4$ ms and $T_C = 7.6$ ms. Phase cycle: $\phi1 = x,-x$, $\phi2 = 4(x),4(-x)$, $\phi3 = 8(x),8(-x)$, $\phi4 = x,-x$, $\phi b1 = 2(x),2(-x)$, $\phi b2 = 2(x),2(y),2(-x),2(-y)$, rec $= 2(x,-x,-x,x),2(-x,x,x,-x)$. Quadrature detection in F_1 is obtained by incrementing $\phi3$ in a States-TPPI manner.[25] The strengths (G/cm) and durations (ms) of gradients are: G0 = (4,0.5), G1 = (5,0.5), G2 = (12,1), G3 = (7,0.3), G4 = (−25,0.5), G5 = (10,0.1), G6 = (15,1), G7 = (2,0.3), Gb1 = Gb2 = (−10,0.4). Figure 1B shows the pulse scheme for the measurement of the relaxation of D1′: The ^{13}C carrier is at 85 ppm. Selective 180° pulses (RE-BURP[23]) denoted by "SU" (on-resonance, 380 μs), "C1′C5" (carrier at 94.3 ppm, 2.4 ms), and "C1′" (92 ppm, 4.1 ms) are applied. The selective pulse "C1′C5" is applied in alternate scans to suppress the transfer of magnetization that originates on H1′/H5. The delays employed are: $\tau_a = \tau_b = 1.7$ ms, $T_C = 13.3$ ms, $T_{C1} = 11.6$ ms, and $T_d = 2.4$ ms. The phase cycle is: $\phi1 = x,-x$, $\phi2 = 4(x),4(-x)$, $\phi3 = 8(x),8(-x)$, $\phi4 = x,-x$, $\phi5 = 2(-y),2(y)$, $\phi b1 = 2(x),2(-x)$, $\phi b2 = 2(y),2(x),2(-y),2(-x)$, rec $= 2(x,-x,-x,x),2(-x,x,x,-x)$ with quadrature detection in F_1 achieved via States-TPPI[25] of $\phi3$. Gradients are as in part A, with G2′ half the duration of G2 (same intensity). Figure 1C shows the pulse scheme for the measurement of relaxation properties of D2′. The ^{13}C carrier is at 85 ppm. Selective 180° pulses (RE-BURP) are denoted by "SU" (on-resonance, 380 μs), "C1′C5" (centered at 94.3 ppm, 2.4 ms), and "C1′" (92 ppm, 4.1 ms) are applied. The delays used are: $\tau_a = 1.59$ ms, $\tau_b = 1.49$ ms, $T_C = 13.3$ ms, $T_{C1} = 11.6$ ms, and $T_{EVLV} = 9.4$ ms. The phase cycle is: $\phi1 = x,-x$, $\phi2 = 4(x),4(-x)$, $\phi3 = 8(x),8(-x)$, $\phi4 = x,-x$, $\phi5 = 2(-y),2(y)$, $\phi6 = x$, $\phi b1 =$

(11) Borer, P. N.; LaPlante, S. R.; Kumar, A.; Zanatta, N.; Martin, A.; Hakkinen, A.; Levy, G. C. *Biochemistry* **1994**, *33*, 2441−2450.
(12) Boisbouvier, J.; Brutscher, B.; Simorre, J. P.; Marion, D. *J. Biomol. NMR* **1999**, *14*, 241−252.
(13) Boisbouvier, J.; Wu, Z.; Ono, A.; Kainosho, M.; Bax, A. *J. Biomol. NMR* **2003**, *27*, 133−142.
(14) Muhandiram, D. R.; Yamazaki, T.; Sykes, B. D.; Kay, L. E. *J. Am. Chem. Soc.* **1995**, *117*, 11536−11544.
(15) Millet, O.; Muhandiram, D. R.; Skrynnikov, N. R.; Kay, L. E. *J. Am. Chem. Soc.* **2002**, *124*, 6439−6448.
(16) Furtig, B.; Richter, C.; Bermel, W.; Schwalbe, H. *J. Biomol. NMR* **2004**, *28*, 69−79.
(17) Lipari, G.; Szabo, A. *J. Am. Chem. Soc.* **1982**, *104*, 4546−4559.
(18) Batey, R. T.; Cloutier, N.; Mao, H.; Williamson, J. R. *Nucleic Acids Res.* **1996**, *24*, 4836−4837.
(19) Kao, C.; Rudisser, S.; Zheng, M. *Methods* **2001**, *23*, 201−205.
(20) Puglisi, J. D.; Wyatt, J. R. *Methods Enzymol.* **1995**, *261*, 323−350.
(21) Delaglio, F.; Grzesiek, S.; Vuister, G. W.; Zhu, G.; Pfeifer, J.; Bax, A. *J. Biomol. NMR* **1995**, *6*, 277−293.
(22) Kamath, U.; Shriver, J. W. *J. Biol. Chem.* **1989**, *264*, 5586−5592.
(23) Geen, H.; Freeman, R. *J. Magn. Reson.* **1991**, *93*, 93−141.
(24) Kupce, E.; Freeman, R. *J. Magn. Reson., Ser. A* **1996**, *118*, 299−303.
(25) Marion, D.; Ikura, M.; Bax, A. *J. Magn. Reson.* **1989**, *84*, 425−430.

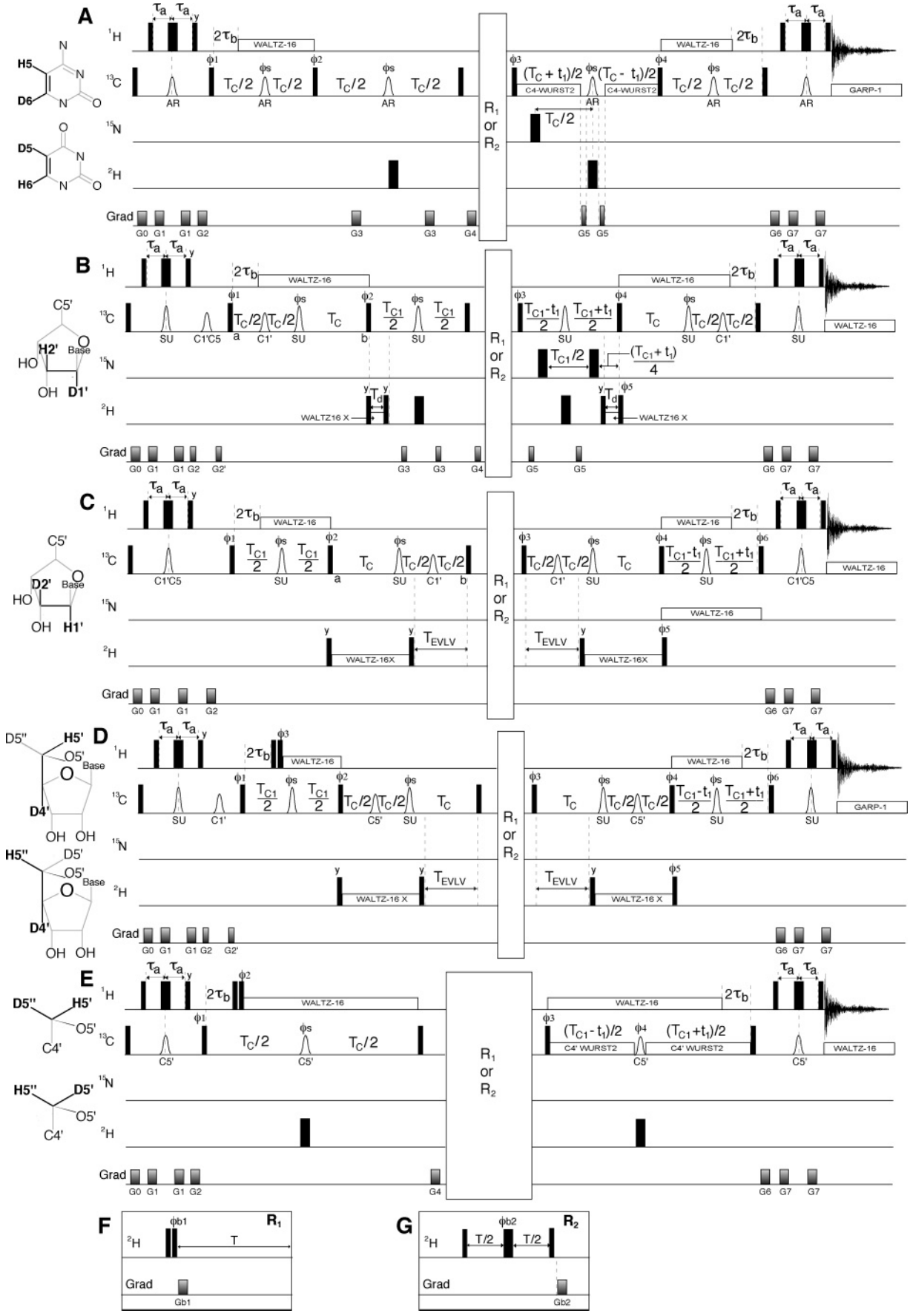

Figure 1. Pulse schemes used to measure ^{2}H R_1 and R_2 relaxation rates at 5,6 base (U,C) and 1′,2′,4′,5′,5″ sugar positions in uniformly ^{15}N, ^{13}C ∼50% ^{2}H labeled RNA. The magnetization transfer pathway is indicated in black along the carbon backbone (gray) of either the base or sugar. Details are given in Materials and Methods.

2(*x*),2(−*x*), ϕb2 = 2(*y*),2(*x*),2(−*y*),2(−*x*), rec = 2(*x*,−*x*,−*x*,*x*),2(−*x*,*x*,*x*,−*x*) with quadrature detection in F_1 achieved by States-TPPI of ϕ6. Gradients are as in part A. Figure 1D shows the sequence for the measurement of dynamics at the D4′ position. Many of the details are as in part C. "C1′" is a 4-ms RE-BURP inversion pulse (centered at 92.2 ppm) applied in alternate scans to suppress magnetization originating from H1′ while shape "C5′" (RE-BURP) is of duration 4.1 ms and is centered at 66.8 ppm. The delays used are: $\tau_a = \tau_b = 1.69$ ms, $T_C = 12.8$ ms, $T_{C1} = 11.6$ ms, and $T_{EVLV} = 9.4$ ms. The phase cycle is: $\phi1 = x,-x$, $\phi2 = 4(x),4(-x)$, $\phi3 = 8(x),8(-x)$, $\phi4 = x,-x$, $\phi5 = 2(-y),2(y)$, $\phi6 = x$, ϕb1 = 2(*x*),2(−*x*), ϕb2 = 2(*y*),2(*x*),2(−*y*), 2(−*x*), rec = 2(*x*,−*x*,−*x*,*x*),2(−*x*,*x*,*x*,−*x*) with quadrature detection in F_1 achieved via States-TPPI of ϕ6. Figure 1E shows the scheme for measurement of relaxation of D5′/D5″. The ^{13}C carrier is placed at 66 ppm with "C5′" a 2-ms RE-BURP pulse centered at 64 ppm. C4′ decoupling is as described in part A with the field centered at 84.5 ppm. The delays used are: $\tau_a = \tau_b = 1.7$ ms, $T_C = 9.5$ ms, and $T_{C1} = 11$ ms. The phase cycle is: $\phi1 = x,-x$, $\phi2 = 8(x),8(-x)$, $\phi3 = x$, $\phi4 = 4(x),4(y),4(-x),4(-y)$, ϕb1 = 2(*x*),2(−*x*), ϕb2 = 2(*x*),2(*y*),2(−*x*), 2(−*y*), rec = *x*,2(−*x*),*x*,−*x*,2(*x*),−*x*. Quadrature detection in F_1 is achieved via States-TPPI of ϕ3. Gradients are as in part A.

RNA Model. A model of the GGCAC−UUCG-GUGCC 14-mer RNA was generated starting from crystal structures containing the **C**-UUCG-**G** stem loop sequence.[26] The C−G base pair of the stem loop X-ray structure (indicated in bold above) was superimposed on a five base pair sequence (standard A form RNA[27]) consisting of the first five base pairs of the 14-mer (GGCAC/GUGCC). Base pairs A4-U11 and C5-G10 in the molecule so formed were minimized using the CHARMM program[28] with a force field optimized for nucleic acids.[29]

Calculations. Expressions for the relaxation of ^{2}H longitudinal and transverse magnetization are well-known:[14,30]

$$R^{Q}(D_Z) = R_1 = \frac{3}{40}\left(\frac{2\pi e^2 qQ}{h}\right)^2 [J(\omega_D) + 4J(2\omega_D)] \quad (1)$$

$$R^{Q}(D_+) = R_2 = \frac{1}{80}\left(\frac{2\pi e^2 qQ}{h}\right)^2 [9J(0) + 15J(\omega_D) + 6J(2\omega_D)] \quad (2)$$

where e^2qQ/h is the quadrupolar coupling constant (QCC) and $J(\omega_D)$ is a spectral density function evaluated at ω_D, the Larmor frequency of ^{2}H. All data have been analyzed using the Lipari−Szabo model free spectral density,[17] which in the case of axially symmetric tumbling becomes:[31]

$$J(\omega) = \sum_{i=0}^{2} A_i \left[\frac{S^2\tau_i}{1 + (\omega\tau_i)^2} + \frac{(1 - S^2)\tau_i^f}{1 + (\omega\tau_i^f)^2}\right] \quad (3)$$

where $A_0 = 0.75 \sin^4 \alpha$, $A_1 = 3 \sin^2 \alpha \cos^2 \alpha$, $A_2 = (3 \cos^2 \alpha - 1)^2/4$, $\tau_0 = (4D_{||} + 2D_\perp)^{-1}$, $\tau_1 = (D_{||} + 5D_\perp)^{-1}$, $\tau_2 = (6D_\perp)^{-1}$, and $(\tau_i^f)^{-1} = (\tau_i)^{-1} + (\tau^f)^{-1}$. Here α is the angle that the bond vector of interest makes with the unique axis of the diffusion tensor, S is an order parameter describing the amplitude of CD bond vector excursions, and τ^f is the correlation time for these rapid motions.

The diffusion tensor was estimated by minimization of χ^2:[32]

$$\chi^2 = \sum_{i=1}^{N} [(R_2^{expt}/R_1^{expt})_i - (R_2^{calcd}/R_1^{calcd})_i]^2/(\sigma_{R_2/R_1})_i^2 \quad (4)$$

using the Levenberg−Marquart algorithm,[33] where the summation extends over all sites for which data is obtained. R_1^{expt} and R_2^{expt} are the experimentally measured rates, R_1^{calcd} and R_2^{calcd} are the rates calculated using diffusion tensor parameters and expressions for R_1, R_2, $J(\omega_D)$ above, and σ_{R_2/R_1} is the uncertainty in the experimental R_2/R_1 value. Reduced χ^2 values of 1.04 (25 °C) and 1.33 (5 °C) were obtained from the fits. A fully anisotropic diffusion tensor was not fit to the data since (i) a structural *model* was employed, (ii) calculations establish that the inertia tensor is axially symmetric, and (iii) low χ^2 values were obtained with the axially symmetric model. In evaluating R_2 and R_1 values above, S^2 has been set to 1 (i.e., only the first term of the spectral density function above was employed). The diffusion tensor parameters estimated by minimizing χ^2 are sensitive to rates measured in regions of the molecule with dynamics that are not properly described by eq 3 or to errors in the structural model used. Because the tetraloop and the first base pair (G1−C14) are expected to be flexible, only rates measured for nucleotides 2−5 and 10−13 were used in the diffusion tensor calculations. Data for several nuclei were eliminated prior to calculation of the diffusion tensor using the following approach.[34] After each round of minimization using

$$\chi = \sum_{i=1}^{N} \chi_i = \sum_{i=1}^{N} |(R_2^{expt}/R_1^{expt})_i - (R_2^{calcd}/R_1^{calcd})_i|/(\sigma_{R_2/R_1})_i \quad (5)$$

The data point with the highest χ_i was eliminated, and the fitting was repeated until there were no points for which $\chi_i > 2.5$. Data for G10 D4′, U11 D5″, G10 D5′, and G2 D5′ were eliminated (25 °C), while U11 D5″, G10 D5′, and C13 D5 were removed from the 5 °C data set. G2, G10, and C13 are adjacent to regions with flexibility, while U11 is at the interface where coordinates from the tetraloop and ideal A-form helix were merged in the model. After elimination of these data points, minimization of either χ^2 or χ gave similar values for the diffusion tensor, and all of the results reported are from the minimization of χ^2. Errors in the fitted parameters (θ, ϕ, $D_{||}$, and $D_\perp$) were estimated by a Monte Carlo procedure in which 500 synthetic data sets were generated by random addition of errors (based on experimental uncertainties) to the measured rates and repeating the fits. The standard deviations in the fitted parameters are used to represent the uncertainties in the parameters.

Motional parameters S^2 and τ^f were obtained by minimizing

$$\chi_{LS}^2 = [(R_1^{expt} - R_1^{calcd})^2/\sigma_{R_1}^2] + [(R_2^{expt} - R_2^{calcd})^2/\sigma_{R_2}^2] \quad (6)$$

for each site for which data is available. The rates were calculated using the expressions for R_1, R_2, and $J(\omega_D)$ above, along with the diffusion tensor parameters. Uncertainties in the fitting parameters were estimated by standard Monte Carlo procedures described above, using the estimated errors for the rates. The relaxation data from several sites could not be well fit to the simple Lipari−Szabo model[17] (U6 D5′, U7 D4′, U11 D5″ at 25 °C; U6 D5′, C8 D5, and U11 D5″ at 5 °C). This may reflect inaccuracies in the model structure used to interpret the relaxation data or the presence of more complex motions that are not accounted for by the motional model that is used.

(26) Ennifar, E.; Nikulin, A.; Tishchenko, S.; Serganov, A.; Nevskaya, N.; Garber, M.; Ehresmann, B.; Ehresmann, C.; Nikonov, S.; Dumas, P. *J. Mol. Biol.* **2000**, *304*, 35−42.
(27) Macke, T. J.; Case, D. A. In *Molecular Modeling of Nucleic Acids*; Leontis, N. B., SantaLucia, J., Jr., Eds.; ACS Symposium Series 682; American Chemical Society: Washington, DC, 1998; pp 379−393.
(28) Brooks, B. R.; Bruccoleri, R. E.; Olafson, B. D.; States, D. J.; Swaminathan, S.; Karplus, M. *J. Comput. Chem.* **1983**, *4*, 187−217.
(29) MacKerell, A. D.; Banavali, N. K. *J. Comput. Chem.* **2000**, *21*, 105−120.
(30) Abragam, A. *Principles of Nuclear Magnetism*; Clarendon Press: Oxford, 1961.
(31) Woessner, D. E. *J. Chem. Phys.* **1962**, *37*, 647−654.
(32) Tjandra, N.; Feller, S. E.; Pastor, R. W.; Bax, A. *J. Am. Chem. Soc.* **1995**, *117*, 12562−12566.
(33) Press, W. H.; Flannery, B. P.; Teukolsky, S. A.; Vetterling, W. T. *Numerical Recipes in C: The Art of Scientific Computing*, 2nd ed.; Cambridge Univerisity Press: New York, 1992.
(34) Hwang, P. M.; Skrynnikov, N. R.; Kay, L. E. *J. Biomol. NMR* **2001**, *20*, 83−88.

Unlike the R_2/R_1 ratio where the value of the QCC is not needed, accurate values are required for the extraction of motional parameters. Literature QCC values of 174 kHz for the sugar deuterons and 179 kHz for D6 were used, based on previous ^{2}H solid-state NMR studies of nucleic acids.[35] The QCC for D5 was not available and therefore was estimated in this study by assuming that base D5 and D6 deuterons in the stem region of the RNA, where internal dynamics are smallest, have the same dynamics parameters. Values of the QCC for each D5 were subsequently obtained from the measured R_1, R_2 values and the orientation of D5 using eqs 1−3. In this manner, a pair of estimates was obtained for each D5. Fourteen values of the QCC were obtained (C3, C5, U11 at 25 and 5 °C, C13 at 25 °C); residues in the more dynamic tetraloop were not used. Average and standard deviations for the QCC of 187.5, 2.5 kHz were obtained, respectively. Very similar values of the QCC were obtained for D5 of C (187.4 ± 2.9 kHz) and U (187.7 ± 1.8 kHz), although in the case of U only data from one residue (four estimates) was available. A value of 187.5 kHz was used to extract dynamics parameters at each D5 site. It is worth noting that the process of estimating the QCC for D5 positions necessarily implies that the order parameters obtained for D5/D6 are not independent for the rigid stem residues (C3,C5,U11,C13). Values of S^2 are not identical at these sites, however, because the QCC value used is an average over many (14) positions. Order parameters for D5/D6 in the interesting loop region are independent, however.

Results and Discussion

Labeling Strategy. In proteins ^{2}H relaxation rates are measured for deuterons of $^{13}CH_2D$ methyl[14] or ^{13}CHD methylene[36] groups that are selected by simple pulse sequence manipulations from the variety of isotopomers generated using uniform ^{13}C labeling and ∼50% fractional deuteration. In the case of RNA, we use the same labeling strategy and measure relaxation in HCD groups at the 5′ position in sugars and in H−C−C−D spin systems in the sugars and pyrimidine bases of uniformly ^{13}C, ∼50% ^{2}H labeled RNA.

NMR Methodology. The pulse schemes used to measure ^{2}H R_1 and R_2 spin relaxation rates at 5,6 U,C aromatic and 1′,2′,4′,5′,5″ sugar positions are shown in Figure 1. In principle, it is straightforward to measure rates at the 3′ position as well, although we have not attempted to do so here. In what follows we briefly describe the magnetization transfer pathways and where appropriate elaborate on the approaches used to ensure the directionality of magnetization flow. Figure 1A shows the sequence used to measure relaxation rates at the D5 and D6 positions of U and C, with the transfer of magnetization summarized by:

$$\mathrm{H5} \xrightarrow{J_{C5H5}} \mathrm{C5} \xrightarrow{J_{C5C6}} \mathrm{C6} \xrightarrow{J_{C6D6}} \mathrm{D6(T)} \xrightarrow{J_{C6D6}} \mathrm{C6}(t_1) \xrightarrow{J_{C5C6}} \mathrm{C5} \xrightarrow{J_{C5H5}} \mathrm{H5}(t_2)$$

and

$$\mathrm{H6} \xrightarrow{J_{C6H6}} \mathrm{C6} \xrightarrow{J_{C5C6}} \mathrm{C5} \xrightarrow{J_{C5D5}} \mathrm{D5(T)} \xrightarrow{J_{C5D5}} \mathrm{C5}(t_1) \xrightarrow{J_{C5C6}} \mathrm{C6} \xrightarrow{J_{C6H6}} \mathrm{H6}(t_2)$$

Thus, magnetization starting on H5(6) is transferred using the one bond ^{1}H5(6)−^{13}C5(6), ^{13}C5(6)−^{13}C6(5), and ^{13}C6(5)−D6(5) couplings to D6(5), where it is manipulated as shown in Figure 1, part F (R_1) or part G (R_2), to create either longitudinal (C_ZD_Z, where C and D are ^{13}C and ^{2}H spin operators, respectively) or transverse (C_ZD_+) ^{2}H magnetization, which is then allowed to relax for time T. On the way back there is a constant-time element where ^{13}C chemical shift is evolved prior to detection of proton magnetization. In this way, a series of two-dimensional data sets are recorded as a function of T with cross-peaks at (ω_{C6},ω_{H5}) and (ω_{C5},ω_{H6}) for each U and C base (Figure 2). It is also possible to record spectra with correlations at (ω_{C5},ω_{H5}) and (ω_{C6},ω_{H6}) by measuring carbon chemical shift immediately prior to the transfer back to protons. Indeed, for many of the sequences either the shift of the destination or origination carbon can be monitored, although where possible we prefer to record the shift of the C1′ carbon to enhance spectral dispersion. Relaxation rates can be extracted directly by fitting the intensity of each peak as a function of T to an exponential decay curve (Figure 2B). It is worth emphasizing that only those molecules with HCCD labeling give rise to signals in the experiment.

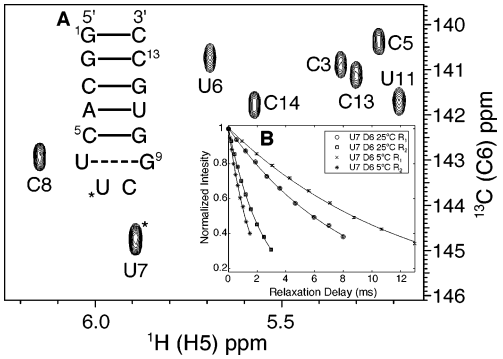

Figure 2. C6−H5 region of the ^{13}C−^{1}H correlation map of the 14-mer indicated in inset A recorded with the scheme of Figure 1A, (T = 50 μs), 600 MHz, 25 °C. Inset B shows R_1 and R_2 curves for the D6 position of U7 (*) measured at 25 and 5 °C.

The magnetization transfer pathways for the measurement of the D1′ (Figure 1B) and D2′ (Figure 1C) relaxation rates are shown below:

$$\mathrm{H2'} \xrightarrow{J_{C2'H2'}} \mathrm{C2'} \xrightarrow{J_{C1'C2'}} \mathrm{C1'} \xrightarrow{J_{C1'D1'}} \mathrm{D1'}(T) \xrightarrow{J_{C1'D1'}} \mathrm{C1'}(t_1) \xrightarrow{J_{C1'C2'}} \mathrm{C2'} \xrightarrow{J_{C2'H2'}} \mathrm{H2'}(t_2)$$

$$\mathrm{H1'} \xrightarrow{J_{C1'H1'}} \mathrm{C1'} \xrightarrow{J_{C1'C2'}} \mathrm{C2'} \xrightarrow{J_{C2'D2'}} \mathrm{D2'}(T) \xrightarrow{J_{C2'D2'}} \mathrm{C2'} \xrightarrow{J_{C1'C2'}} \mathrm{C1'}(t_1) \xrightarrow{J_{C1'H1'}} \mathrm{H1'}(t_2)$$

Because the C2′ and C3′ chemical shifts are not well-resolved, we have used a constant-time element set to $1/J_{CC}$, where J_{CC} is the one-bond ^{13}C2′−^{13}C3′ coupling (duration 2 T_c, from a to b in Figure 1B,C) so that net evolution due to $J_{C2'C3'}$ does not occur. In contrast, the selective C1′ 180° pulse applied in the middle of one of the T_c periods ensures that evolution due to ^{13}C1′−^{13}C2′ does proceed for a net period of $0.5/J_{CC}$.[37] Data sets with correlations at ($\omega_{C1'}$,$\omega_{H2'}$) and ($\omega_{C1'}$,$\omega_{H1'}$) are obtained for measurement of D1′ and D2′ rates, respectively. A similar transfer scheme is employed for the measurement of the

(35) Kintanar, A.; Alam, T. M.; Huang, W. C.; Schindele, D. C.; Wemmer, D. E.; Drobny, G. *J. Am. Chem. Soc.* **1988**, *110*, 6367−6372.
(36) Yang, D.; Mittermaier, A.; Mok, Y. K.; Kay, L. E. *J. Mol. Biol.* **1998**, *276*, 939−954.
(37) Hoogstraten, C. G.; Pardi, A. *J. Magn. Reson.* **1998**, *133*, 236−240.

relaxation properties of D4′ (Figure 1D), with magnetization originating on H5′ or H5″ prior to the transfer to D4′:

$$\mathrm{H5'/H5''} \xrightarrow{J_{C5'H5''}/J_{C5'H5''}} \mathrm{C5'} \xrightarrow{J_{C5'C4'}} \mathrm{C4'} \xrightarrow{J_{C4'D4'}} \mathrm{D4'}(T) \xrightarrow{J_{C4'D4'}} \mathrm{C4'} \xrightarrow{J_{C5'C4'}} \mathrm{C5'}(t_1) \xrightarrow{J_{C5'H5'}/J_{C5'H5''}} \mathrm{H5'/H5''}(t_2)$$

Spectra are therefore obtained with correlations at ($\omega_{C5'}$,$\omega_{H5'}$) and ($\omega_{C5'}$,$\omega_{H5''}$), providing two independent measures of D4′ relaxation rates.

Figure 1E shows the pulse scheme used to measure R_1 and R_2 relaxation rates for D5′ and D5″. The experiment employed is very similar to our previous sequence for the measurement of deuterium relaxation in ^{13}CHD methylenes in proteins[36] and to an experiment that was developed subsequently for quantification of ^{2}H spin relaxation in ^{13}CHD groups of nucleic acids.[38] Differences relative to other ^{13}CHD sequences include selective INEPT transfers[39] that limit the spectral width necessary in the indirect detection dimension, as well as delays and decoupling trains that are optimal for applications to RNA molecules. The transfer of magnetization is summarized by:

$$\mathrm{H5'/H5''} \xrightarrow{J_{C5'H5''}/J_{C5'H5''}} \mathrm{C5'} \xrightarrow{J_{C5'D5''}/J_{C5'D5'}} \mathrm{D5''/D5'}(T) \xrightarrow{J_{C5'D5''}/J_{C5'D5'}} \mathrm{C5'}(t_1) \xrightarrow{J_{C5'H5''}/J_{C5'H5''}} \mathrm{H5'/H5''}(t_2)$$

with transfer from H5′ and H5″ occurring simultaneously. Cross-peaks at ($\omega_{C5'}$,$\omega_{H5'}$) and ($\omega_{C5'}$,$\omega_{H5''}$) report on the relaxation of D5″ and D5′, respectively.

Deuterium Relaxation Rates. The experiments described above have been used to measure relaxation rates at 13 D1′, 10 D2′, 9 D4′, 7 D5′, 10 D5″ (out of a total of 14 sites; see Supporting Information Table 1), and at all 8 D5 and 8 D6 positions (C and U), 25 °C. At 5 °C, rates were measured at 10 D2′, 6 D5′, 12 D5″, 8 D5, and 8 D6 sites. Errors in the relaxation data, estimated on the basis of repeat measurements, were less than 2%, on average. As described above, all of the pulse schemes measure the relaxation of elements of the form C_ZD_Z or C_ZD_+, rather than deuterium longitudinal or transverse operators, D_Z or D_+. The relaxation rates obtained can be "converted" into pure ^{2}H rates by subtraction of $R_1(C_Z)$ from each of the measured values.[14] In practice, however, the correction is small. For example, $R(C_ZD_Z)$ varies between 120 and 175 s^{-1} at 25 °C and between 73 and 107 s^{-1} at 5 °C, with $R(C_ZD_+)$ between 362 and 576 s^{-1} and 613−922 s^{-1} at 25 and 5 °C, respectively (Supporting Information Table 1). $R_1(C_Z)$ values tend to be very similar for each type of nucleus and range from 0.7 to 2.8 s^{-1} at 25 °C and between 0.6 and 1.6 s^{-1} at 5 °C. Neglect of the correction described above will affect the rates by a maximum of 2%, while the sequence-dependent variation in the relaxation values is much larger than 2%. Although we have made the correction to the data recorded here, in general this will not be necessary.

As described previously in connection with the measurement of ^{2}H spin relaxation in methyl groups, one of the powerful features of using the deuteron to probe dynamics is that it is possible to establish the consistency of the experimental data prior to its analysis in terms of motional parameters.[15] Because the deuteron is a spin 1 particle, there are five relaxation rates that can be probed. Jacobsen et al. have derived the following conditions for these five relaxation rates:[40]

$$R^Q(D_Z) \le \frac{5}{3}R^Q(D_+{}^2) \le \frac{5}{3}R^Q(3D_Z{}^2 - 2) \le R^Q(D_+) \le \frac{5}{3}R^Q(D_+D_Z + D_ZD_+) \quad (7)$$

$$R^Q(D_+D_Z + D_ZD_+) = R^Q(D_+) - \frac{2}{3}R^Q(3D_Z{}^2 - 2) \quad (8)$$

$$R^Q(D_+{}^2) = \frac{1}{2}R^Q(D_Z) + \frac{1}{6}R^Q(3D_Z{}^2 - 2) \quad (9)$$

where $R^Q(D_Z) = R_1$ and $R^Q(D_+) = R_2$ are the longitudinal and transverse ^{2}H relaxation rates and $R^Q(3D_Z{}^2 - 2)$, $R^Q(D_+{}^2)$, and $R^Q(D_+D_Z + D_ZD_+)$ correspond to the relaxation rates of quadrupolar order, double quantum, and anti-phase single quantum elements, respectively. Values for the later three (rank-2) rates have been measured for D5′ and D5″ by modifying the pulse sequence of Figure 1E as described by Millet et al.[15] These experiments are significantly less sensitive than those that quantify R_1 and R_2 since longer delays are required for the transfer of magnetization from ^{13}C to ^{2}H, with ^{2}H spin flips degrading the quality of transfer. This is particularly the case in the present example (relative to applications involving methyl groups) because of the very short ^{2}H T_1 values (typically on the order of 11.5 and 7 ms at 5 and 25 °C, respectively). Nevertheless, all five rates have been obtained for a number of residues, and while the errors in the rank-2 data are significant (∼15%), the inequality relation above (eq 7) is satisfied at each position (Figure 3A). Because the errors in rank-2 rates are large in relation to the range of values measured, the two linear consistency relations above (eqs 8 and 9) are less informative. We prefer, therefore, to use rates measured on a concentrated mixture of partially digested nucleotides (∼50 mM). The C5′−H5′/H5″ region of the spectrum of the digest contains four well-resolved correlations, and rates were measured at 25, 12.5, and 5 °C for these four peaks, with the measurement at 5 °C repeated after addition of 40% glycerol to the sample to increase the correlation time. The equality relations are satisfied over the entire range of data (Figure 3B,C), confirming that deuterium relaxation in RNA is dominated by the quadrupolar mechanism and that the data are robust (at least for D5′/D5″).

Diffusion Anisotropy. Previous solid-state NMR studies have established that the quadrupolar tensors of deuterons in C−D spin systems are axially symmetric with the unique axis lying along the CD bond vector.[7,41,42] In the case of nonspherical molecules the measured relaxation rate at a given position will depend, therefore, on the orientation of the CD bond with respect to the diffusion tensor of the molecule. Prior to obtaining measures of internal dynamics, it is necessary to establish the diffusion parameters. Since a structure of the RNA studied is not available, a model has been constructed on the basis of the known structures of UUCG tetraloops[26] and standard A-form RNA (see Materials and Methods). The relative moments of inertia of the RNA model are 1.0, 0.98, and 0.50, showing that

(38) Maltseva, T. V.; Foldesi, A.; Chattopadhyaya, J. *Magn. Reson. Chem.* **1999**, *37*, 203-213.
(39) Morris, G. A.; Freeman, R. *J. Am. Chem. Soc.* **1979**, *101*, 760−762.
(40) Jacobsen, J. P.; Bildsoe, H. K.; Schaumburg, K. *J. Magn. Reson.* **1976**, *23*, 153−164.
(41) Alam, T. M.; Drobny, G. P. *Chem. Rev.* **1991**, *91*, 1545−1590.
(42) Mantsch, H. H.; Saito, H.; Smith, I. C. P. *Prog. Nucl. Magn. Reson. Spectrosc.* **1977**, *11*, 211−271.

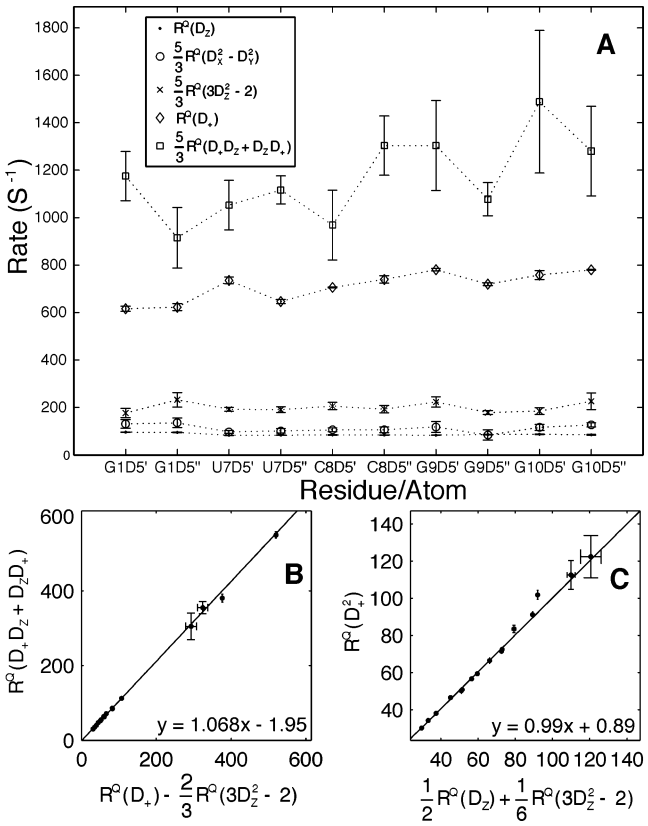

Figure 3. Consistency of the measured ^{2}H relaxation rates. The five deuterium rates measured at well-resolved D5′/D5″ sites of the 14-mer RNA (Figure 2A) satisfy the inequality relations in eq 7. Consistency relations (eqs 8 and 9) are well-satisfied on the basis of measurements of the relaxation properties of well-resolved D5′/D5″ sites recorded on a concentrated solution of a mixture of partially digested nucleotides in D_2O at 25, 12.5, and 5 °C and in D_2O/40% gylcerol, 5 °C. The best fit line to each of the correlations in B and C is indicated.

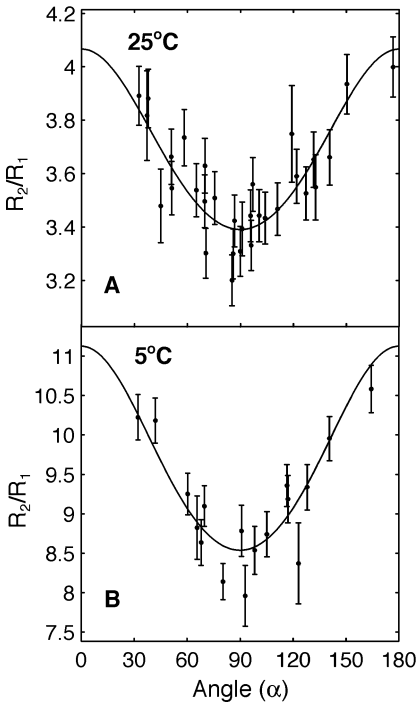

Figure 4. Determination of the molecular diffusion tensor. Plots of R_2/R_1 as a function of the angle α that each of the CD bond vectors makes with respect to the unique angle of the diffusion tensor, along with best fits of the data. Values for θ, ϕ, $R = D_{||}/D_{\perp}$ and τ_c are 21 ± 4°(10 ± 4°), 235 ± 10°(250 ± 31°), 1.35 ± 0.05(1.36 ± 0.05), and 2.74 ± 0.01(5.43 ± 0.03) ns at 25 °C(5 °C), where θ and ϕ are the polar angles describing the orientation of the unique axis of the diffusion tensor with respect to the principal inertial system of the molecule.

it is axially symmetric. Thus, we chose to fit an axially symmetric diffusion tensor, with angles θ and ϕ defining the orientation of the unique axis of the tensor with respect to the inertial frame and $D_{||}$, $D_{\perp}$, the principal components of the diffusion tensor. Independent diffusion tensors at 25 and 5 °C were calculated from R_1 and R_2 relaxation rates measured at the two temperatures, as described above (Figure 4). The large amount of data collected for each nucleotide results in a large sampling of α values (the angle between the bond vector and the unique axis of the diffusion tensor, range of ∼140°), so that the diffusion tensor at each temperature can be defined reasonably well, even with an approximate model. Values of $R = D_{||}/D_{\perp}$ and $\tau_c = (4D_{\perp} + 2D_{||})^{-1}$ of 1.35 ± 0.05(1.36 ± 0.05) and 2.74 ± 0.01(5.43 ± 0.03) are obtained at 25 °C (5 °C) (see legend to Figure 4). These values are consistent with $R = 1.34 \pm 0.12$ measured from ^{15}N relaxation experiments focusing on the imino protons[10] and with $R = 1.39$ from hydrodynamics calculations[43] using a radius of 2.8 Å for each heavy atom. Notably, the ratio of τ_c values at 25 and 5 °C is exactly as expected based on the temperature dependence of the viscosity of D_2O and the Stokes−Einstein equation.

Dynamics in the RNA Molecule. The evolution of a spin 1 particle is described in terms of five independent operators (in addition to the identity operator) that relax with distinct rates. Here we have presented pulse schemes for measuring two of them: the longitudinal and transverse relaxation rates. In addition, rates for the other three elements have been obtained for D5′,D5″ to establish that the measurements at these positions are consistent (see above). In general, the sensitivity of these experiments is significantly worse (by a factor of approximately 10) than for those quantifying the decay of deuterium longitudinal and transverse elements, and we have chosen not to include measured $R^Q(3D_Z^2 - 2)$, $R^Q(D_+^2)$, and $R^Q(D_+D_Z + D_ZD_+)$ values in analyses, beyond establishing the consistency of the data.

The relaxation rates can be related to local molecular dynamics, including an order parameter describing the amplitude of CD bond vector excursions, denoted by S, and τ^f, the correlation time for these rapid (picosecond−nanosecond) motions. Values of S^2 and τ^f were extracted on a per-residue basis using optimized values for the diffusion tensor as fixed parameters (see Materials and Methods). Figure 5 shows the values of S^2 extracted as a function of position in the 14-mer. Notably, the ends of the molecule are more flexible than the central helix, as expected. For example, the 5′,5″ positions at the 5′ end of the RNA are completely unconstrained, and this is reflected in the very low order parameters obtained at these sites (G1). Varani et al. have shown in structural studies of very similar sequences that the β,γ torsion angles between G1 and G2 fluctuate,[44] accounting for the lower-than-average S^2 values for D5′ (0.76),D5″(0.79) of G2 [relative to averages of 0.82 (D5′; averaged over G10 and the loop) and 0.85 (D5″; averaged

(43) Fernandes, M. X.; Ortega, A.; Lopez Martinez, M. C.; Garcia de la Torre, J. *Nucleic Acids Res.* **2002**, *30*, 1782−1788.

(44) Varani, G.; Cheong, C.; Tinoco, I., Jr. *Biochemistry* **1991**, *30*, 3280−3289.

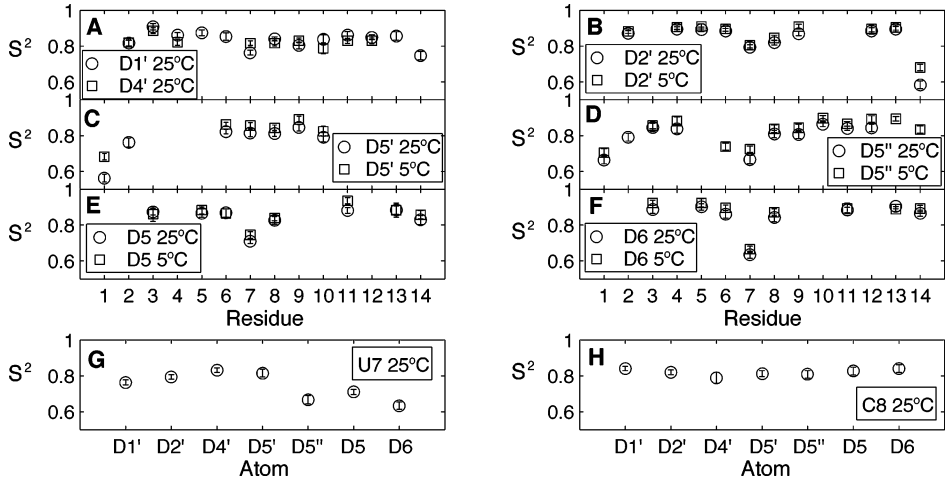

Figure 5. S^2 as a function of sequence in the 14-mer RNA (A−F). S^2 values obtained for U7 and C8 as a function of position in the nucleotide are shown in (G, H).

over the helix residues, excluding G2 and the first base pair)]. Moreover, these authors noted that the first and last sugars exchange between C2′- and C3′-endo conformations,[44] consistent with the observations about order from this study. Interestingly, the order parameters for D5 and D6 at the 3′ end of the molecule (C14; corresponding data at the 5′ end is not available) are high, indicating that, unlike some of the sugar positions at the 3′ terminus, the base CD bonds are relatively rigid. Modest decreases in order (S^2) are observed at the 1′, 2′, and 4′ positions of residues in the tetraloop (U6−G9) in relation to the corresponding positions in the stem (−0.03, on average). Larger deviations are noted for the base 5 and 6 CD bonds of the tetraloop (−0.10), in particular for U7 (−0.21). Crystal and NMR structures of UUCG tetraloops have shown that the U7 base is not stacked and does not make any contacts with the remaining RNA.[26,44,45] U7 adopts slightly different conformations in a pair of crystal structures,[26] and the data presented here establish that the base portion is flexible in solution. In contrast, C8 is constrained by hydrogen-bonding interactions (although it is not base-paired, see below), and consequently, measured D5/D6 S^2 values for this base are similar to those for others. Not surprisingly, therefore, the dynamics across U7 are larger than throughout C8 (Figure 5G,H). The order parameters at 5 °C are almost always higher than those at 25 °C (four exceptions all within error), consistent with expectations.

Values of τ^f vary between 0 and 300 ps for all but one site in the RNA. Interestingly, a value of $\tau^f = 950 \pm 350$ ps was obtained for the C4′D4′ bond of G10. In the crystal structure of an RNA molecule containing a pair of UUCG tetraloops, the β and γ angles that would correspond to those associated with G10 in the structure studied here differ by 35 and 65°, respectively, between the two copies.[26] Thus, the τ^f reported may well correspond to the time scale for the interconversion between the two different conformers that are observed in the crystal.

What Can We Learn, in General, about RNA Dynamics from the Present Work? It is instructive to compare the results of this study with the large database of protein dynamics that has been accumulated over the past decade.[46] The average S^2 value (25 °C) that is obtained for the rigid portion of the 14-mer (residues 2−5 and 10−13) is 0.86 ± 0.04, similar to what has been measured in helices (0.88 ± 0.07), β-structures (0.85 ± 0.07), and turns (0.85 ± 0.09) in proteins. Loop regions in proteins tend to be slightly more dynamic (0.81 ± 0.11), and for the RNA studied here we observe this as well (0.81 ± 0.06 for 6−9). Finally, $S_{avg}^2 = 0.71 \pm 0.13$ for the terminal sites (1 and 14), similar to values measured for termini in proteins (0.61 ± 0.24). The lack of significant dynamics, on average, in this molecule reflects the fact that the RNA is largely a well-structured A-form helix (that appears to be as rigid as elements of regular secondary structure in proteins). The UUCG tetraloop, with the exception of U7, is also relatively rigid. Notably, the order parameters for the U6−G9 base pair are similar to Watson−Crick base pairs in the 14-mer (U6 D5″ is the only exception). In this regard, an ^{15}N spin relaxation study of the imino positions in the RNA established that the base of G9 was the highest ordered, although the results were semiquantitative due to uncertainties in ^{15}N chemical shift anisotropy values.[10] As discussed above, position C8 in the tetraloop is not base-paired but does stack on U6, and order parameters for both sugar and base positions of this nucleotide suggest that it is well-ordered. Correspondingly, in a recent study of base flexibility in the complex of HIV-2 TAR RNA with argininamide, Williamson and co-workers have noted that with the exception of U25 which extends into solution, other bulge nucleotides that are not part of A-form helix or Watson−Crick base pairs are also reasonably rigid.[47] Finally, the dynamics observed in the second position of the UUCG tetraloop studied here have also been noted for a GAAA tetraloop in a ^{13}C $R_{1\rho}$ relaxation study, while the measured relaxation rates of G1 and A3 were similar to those from other well-structured regions of the RNA.[48] Together, these two studies, along with the one presented here, suggest that Watson−Crick base pairing is not necessary to confer order. The importance of NMR studies of RNA dynamics is underscored by the fact that on the basis of X-ray studies it

(45) Allain, F. H.; Varani, G. *J. Mol. Biol.* **1995**, *250*, 333−353.

(46) Goodman, J. L.; Pagel, M. D.; Stone, M. J. *J. Mol. Biol.* **2000**, *295*, 963−978.

(47) Dayie, K. T.; Brodsky, A. S.; Williamson, J. R. *J. Mol. Biol.* **2002**, *317*, 263−278.

(48) Hoogstraten, C. G.; Wank, J. R.; Pardi, A. *Biochemistry* **2000**, *39*, 9951−9958.

was concluded that U7 of the UUCG loop was no more mobile than other residues of the structure,[26] in contrast to what is observed in solution.

Although it is difficult to relate RNA function with dynamics given the paucity of dynamics data on these molecules, it is noteworthy that UNCG tetraloops are thought to be much less involved in RNA or protein recognition than GNRA loops, and these differences have been attributed to a diversity in the dynamics of the two.[49] The rigidity of UNCG sequences may limit their ability to specifically recognize targets that more flexible GNRA constructs are able to bind. A correlate between mobility and function has also been noted in the HIV-2 TAR RNA[47] and in the leadzyme.[48] It is also of interest that the UUCG tetraloop is remarkably stable,[50,51] and this stability may be due to the large enthalpic contribution that derives from a well-ordered structure.

It is important to emphasize that the present study provides a comprehensive set of order parameters that can be used to develop motional models. Although values of S^2 can be analyzed in a simple way in terms of dynamics about one or two torsion angles,[10] for example, such interpretations necessarily exaggerate the extent of motion since all of the dynamics must be accounted for by a (very) small number of degrees of freedom. Instead, order parameters can be used as restraints in molecular dynamics simulations, in concert with other data such as coupling constants, dipolar couplings, and NOEs to obtain an ensemble of structures that satisfy both structural and dynamics constraints.[52,53] This provides a convenient way of "visualizing" the extent of dynamics and serves as an entry point for the calculation of thermodynamic parameters[54] in ways that we believe are more rigorous than what is currently done from NMR-derived order parameters.[55−57] This work is now in progress.

Concluding Remarks

A set of relaxation experiments for obtaining accurate ^{2}H R_1 and R_2 rates at a wide variety of sites in RNA molecules has been presented. The methodology is applied to a small 14-mer at 25 and 5 °C. Interestingly, the relative sensitivities of relaxation experiments recorded at 25 and 5 °C are similar even though the correlation time increases by a factor of 2 (2.7−5.4 ns). This is likely the result of the compensation between the decreased ^{13}C T_2 values at lower temperature (which decreases the signal/noise) and the increased ^{2}H T_1 values that facilitate magnetization transfer from ^{13}C to ^{2}H. This suggests that applications of the methodology to higher molecular weight RNAs will be successful. For example, the τ_c value estimated for the 30-nucleotide HIV-2 TAR-arginamide complex is 5.2 ns at 25 °C (scaled from the reported value of 4.2 ns in H_2O [47] to account for different solvent viscosities between D_2O and H_2O), within the range of values that have been examined in the present study. It is anticipated, therefore, that the experiments presented will facilitate the study of dynamics in a range of systems, opening up the possibility for quantifying the relation between motion and function in this important class of molecule.

Acknowledgment. This research was supported by grants from the Canadian Institutes of Health Research and the Natural Sciences and Engineering Research Council of Canada. Useful discussions with Profs. H. Schwalbe (Frankfurt) and G. Varani (Seattle) are acknowledged. Profs. R. Collins and J. Forman-Kay provided us with laboratory facilities for the RNA synthesis. We are grateful to Duane Smith and Dr. Dmitry Korzhnev for advice on gel purification of RNA and on analyzing relaxation data, respectively.

Supporting Information Available: List of relaxation delays used to record the ^{2}H decay rates, one table listing the values of ^{2}H R_1, R_2, and ^{13}C R_1 as a function of position in the 14-mer, 25 and 5 °C, and one table listing the motional parameters obtained from the relaxation data. This material is available free of charge via the Internet at http://pubs.acs.org.

JA0427799

(49) Varani, G. *Annu. Rev. Biophys. Biomol. Struct.* **1995**, *24*, 379−404.
(50) Antao, V. P.; Tinoco, I., Jr. *Nucleic Acids Res.* **1992**, *20*, 819−824.
(51) Tuerk, C.; Gauss, P.; Thermes, C.; Groebe, D. R.; Gayle, M.; Guild, N.; Stormo, G.; d'Aubenton-Carafa, Y.; Uhlenbeck, O. C.; Tinoco, I.; Brody, E. N.; Gold, L. *Proc. Natl. Acad. Sci. U.S.A.* **1988**, *85*, 1364−1368.
(52) Lindorff-Larsen, K.; Best, R. B.; Depristo, M. A.; Dobson, C. M.; Vendruscolo, M. *Nature* **2005**, *433*, 128−132.
(53) Best, R. B.; Vendruscolo, M. *J. Am. Chem. Soc.* **2004**, *126*, 8090−8091.
(54) Brooks, B. R.; Janezic, D.; Karplus, M. *J. Comput. Chem.* **1995**, *16*, 1522−1542.
(55) Li, Z.; Raychaudhuri, S.; Wand, A. J. *Protein Sci.* **1996**, *5*, 2647−2650.
(56) Yang, D.; Kay, L. E. *J. Mol. Biol.* **1996**, *263*, 369−382.
(57) Akke, M.; Bruschweiler, R.; Palmer, A. G. *J. Am. Chem. Soc.* **1993**, *115*, 9832−9833.